

Supplementary information

A computational study of the influence of nanoparticle shape on clathrin-mediated endocytosis

Ye Li,^{a,b,c,*} Man Zhang,^{a,b,c} Yezhuo Zhang,^{a,b,c} Xinhui Niu,^{a,b,c} Zhendan Liu,^{a,b,c}

Tongtao Yue^d and Wen Zhang^{a,b,c}

^aState Key Laboratory of Tree Genetics and Breeding, College of Biological Sciences and Technology, Beijing Forestry University, Beijing 100083, China

^bKey Laboratory of Genetics and Breeding in Forest Trees and Ornamental Plants, Ministry of Education, College of Biological Sciences and Technology, Beijing Forestry University, Beijing 100083, China

^cThe Tree and Ornamental Plant Breeding and Biotechnology Laboratory of National Forestry and Grassland Administration, College of Biological Sciences and Technology, Beijing Forestry University, Beijing 10083, China

^dInstitute of Coastal Environmental Pollution Control, Key Laboratory of Marine Environment and Ecology, Ministry of Education, Ocean University of China, Qingdao 266100, China

*Corresponding author: Ye Li (liye0223@bjfu.edu.cn);

Table S1 The interaction parameters (a_{ij}) between different species beads. The subscript of a_{ij} denotes different types of beads in the system, with H lipid head, T lipid tail, R_H receptor head, R_T receptor tail, C_L the shorter light chain bead of clathrin, C_H the longer heavy chain bead of clathrin, P the bead of nanoparticle, H the ligand of nanoparticle and W the water.

i j	H	T	R_H	R_T	P	H	C_L	C_H	W
H	25	50	25	50	25	25	15	15	25
T		15	50	15	50	80	50	50	80
R_H			25	50	25	0	15	15	25
R_T				15	50	80	50	50	80
P					25	25	25	25	25
H						25	25	25	25
C_L							15	10	25
C_H								35	25
W									25

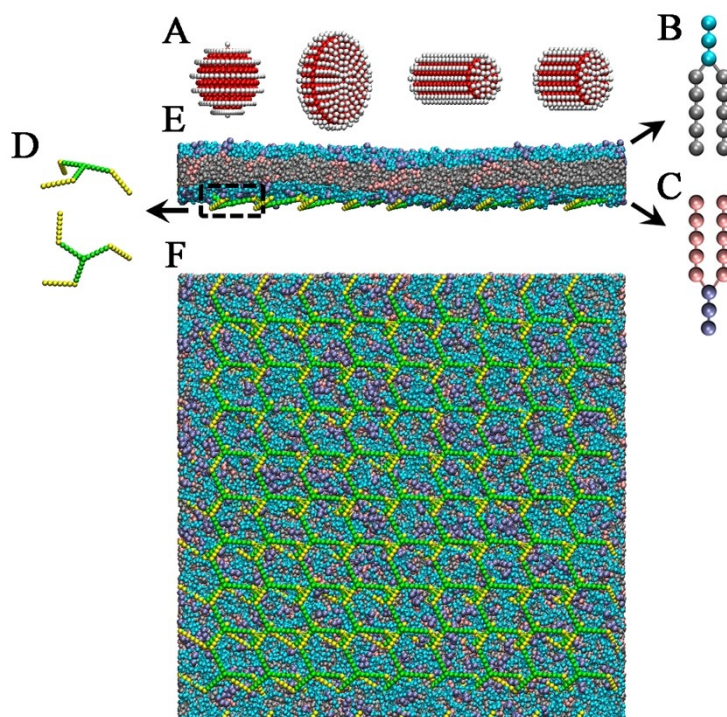


Fig. S1 Schematic diagram of different components (A, B, C, D) and the initial configuration (E, F) in our simulation system. (A) Nanoparticle, (B) Lipid, (C) Ligand, (D) Clathrin.

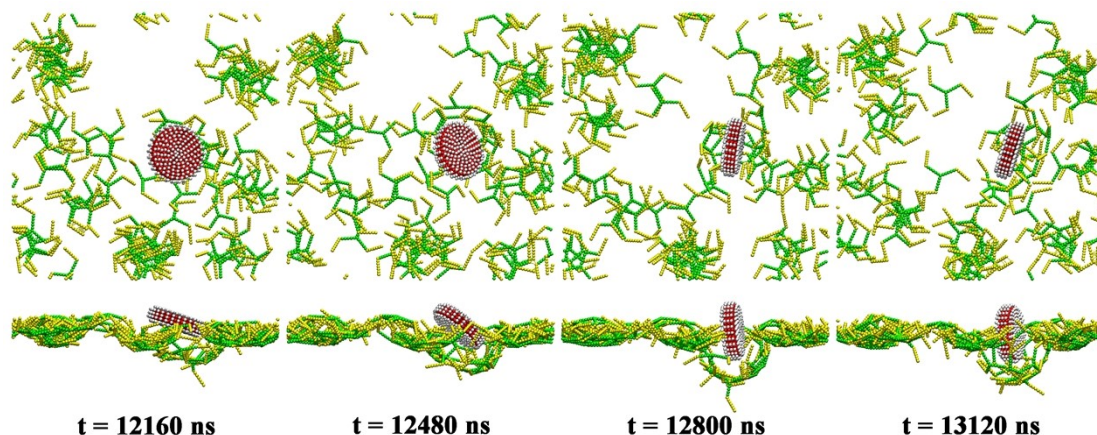


Fig. S2 The rotation for disk-shaped nanoparticle during the wrapping stage. Several typical snapshots for clathrin-mediated endocytosis of disk-shaped NP ($\theta_0=90^\circ$). The lipid membrane and solvent molecules were not shown for clarity.

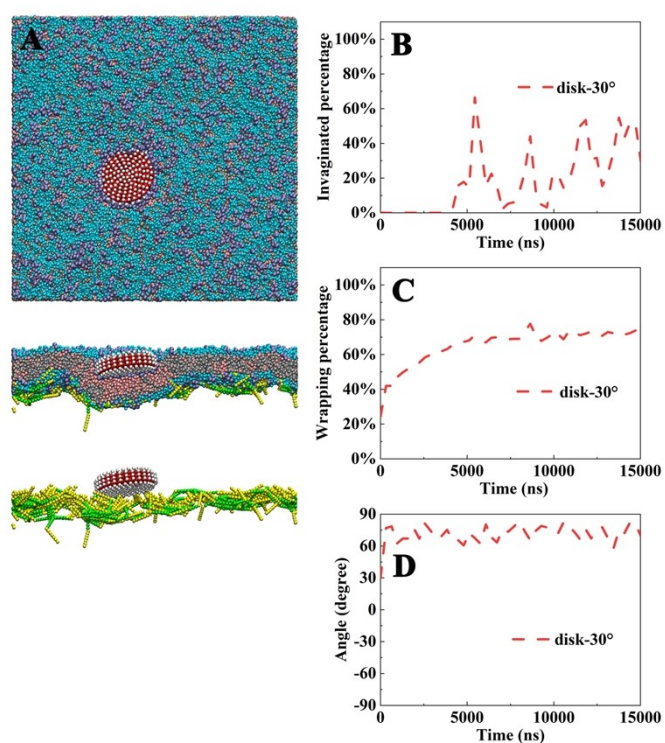


Fig. S3 Clathrin-mediated endocytosis for disk-shaped NP with initial angle of 30° ($D=9.7$ nm and $H=1.9$ nm). (A) Final snapshots of membrane wrapping of disk-shaped NPs from top, cross-sectional views, and only clathrin and NP. (B) Percentage of invagination as a function of time. (C) Percentage of wrapping as a function of time. (D) Evolution of disk-shaped NP orientation angle.

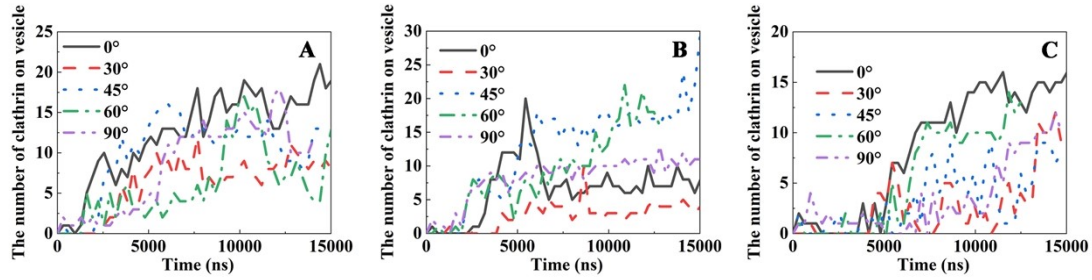


Fig. S4 The number of clathrin on endocytosis vesicle as a function of time during NP wrapping. (A) Long rod-shaped NPs with the different initial orientation angles. (B) Short rod-shaped NPs with the different initial orientation angles. (C) Disk-shaped NPs with the different initial orientation angles.

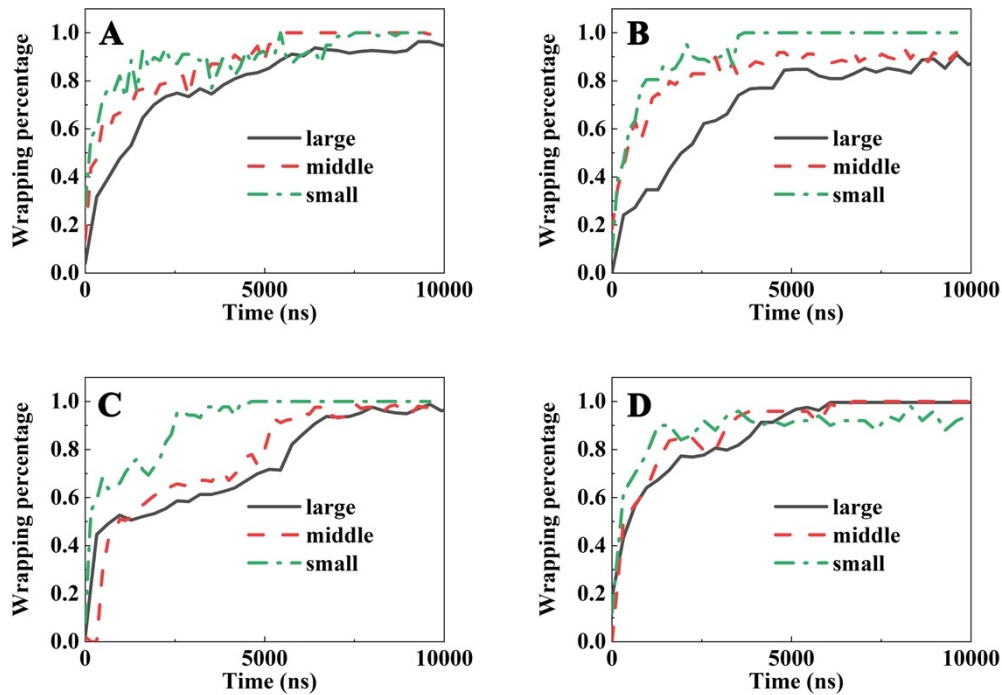


Fig. S5 Clathrin-mediated endocytosis for NPs with different sizes. (A) Percentage of wrapping as a function of time for long rod-shaped NPs with different sizes. Large NP ($D=4.5$ nm, $L=9.7$ nm), middle NP ($D=3.2$ nm, $L=8.4$ nm), small NP ($D=1.9$ nm, $L=7.1$ nm). (B) Percentage of wrapping as a function of time for short rod-shaped NPs with different sizes. Large NP ($D=5.8$ nm, $L=5.8$ nm), middle NP ($D=4.5$ nm, $L=4.5$ nm), small NP ($D=3.2$ nm, $L=3.2$ nm). (C) Percentage of wrapping as a function of time for disk-shaped NPs with different sizes. Large NP ($D=9.7$ nm, $L=1.9$ nm), middle NP ($D=7.1$ nm, $L=1.9$ nm), small NP ($D=4.5$ nm, $L=1.3$ nm). (D) Percentage of wrapping as a function of time for sphere NPs with different sizes. Large NP ($D=7.1$ nm), middle NP ($D=4.5$ nm), small NP ($D=3.2$ nm).